John Vanderkooy
University of Waterloo
Waterloo, Ontario, Canada N2L 3G1

Presented at the 103rd Convention 1997 September 26–29 New York

AES

AN AUDIO ENGINEERING SOCIETY PREPRINT

Loudspeaker Ports

by John Vanderkooy
Audio Research Group, Dept. of Physics,
University of Waterloo
Waterloo ON Canada N2L 3G1
e-mail: jv@audiolab.uwaterloo.ca

Abstract

The demand for high-level low-frequency sound in cinema and home theatre audio systems, and the desire for compact subwoofers, is the motivation behind this work. Tapered ports were believed to perform better than simple ones, and this study sets out to measure and analyze such ports and assess their performance. A model of an acoustic port of varying cross-section is presented. Acoustic ports of various shapes are studied to show their behaviour at a range of levels. It is found that flared ends do help, but at high levels, some losses and distortion remains. A gently-tapered port shows better behaviour.

Introduction

An acoustic port has been a common device to achieve more low-frequency output in loudspeakers. The output of a driver in a box can be augmented in the frequency region where its output is rolling off, by using a properly tuned port. Such vented-box or reflex enclosures have been analyzed by N.Thiele and R.H.Small [1]. Subwoofers can also be designed with coupled-cavity configurations, in which the port is the sole source of the sound that emerges. As sound levels rise, the air velocity in the port increases, until ultimately there is too much distortion or aerodynamic noise from the port. The last few years have seen a growing demand for very high low-frequency sound levels in cinema and home theatre systems, and this paper attempts to study the effects of high sound levels on the operation of acoustic ports. There has been an extensive study by Backman [2] which presents measurements of some interesting configurations, but an understanding of the mechanisms in place is not part of the study, and tapered ports are not considered.

Although subwoofers can be built with direct radiators, their efficiency is too low to be practical, and so the resonant properties of a port and an associated volume of air are usually employed.

The passive radiator is an alternative to a simple port, and has some advantages, but it is more costly. The acoustic port is expected to remain in use, and the purpose of this paper is to study several aspects of its operation.

When sound levels become high, the velocity of the air becomes high, and turbulence occurs, especially near any sharp edges or protrusions. Such turbulence can be heard in actual systems at high levels. Hence all edges should be smooth, and the curved contours of the shape should be as gentle as possible. An optimum port will have the gentlest flare allowable under the circumstances, since this will result in the least inertial forces perpendicular to the axis of the port. Such inertial forces tend to induce turbulence at edges.

What is the optimum design for a port? What would be an optimum design for the subwoofer? Such questions really don't have an answer, but we shall assume that, for a specific acoustic volume V whose determination is not included in the scope of this paper, a single port is required with a specific resonance frequency. The area of the port is thus unspecified, and can be adjusted, under some constraints to be given later, to give adequately low losses, and to attenuate sufficiently the extraneous midrange frequencies inside the box. A single larger port is better than two or more smaller ports having the same resonance frequency, since the single port has less perimeter, with less chance for turbulence due to the shearing of the air flow at the surface.

Acoustic Behaviour of Non-cylindrical Ports

Let us first review the resonance properties of a port consisting of a normal, cylindrical tube of cross-sectional area A and length L, which is coupled to a box of volume V. The mass M of the air in this port is

$$M = \rho A L \tag{1}$$

where ρ is the density of the air. If the "plug" of incompressible air in the port moves out a samll distance dx, the volume change dV is

$$dV = A\, dx \tag{2}$$

and the pressure change for an adiabatic proces (no heat transfer) is

$$dP = -\gamma Po\, dV / V = -\gamma Po\, A\, dx / V \tag{3}$$

where Po is atmospheric pressure and $\gamma = 7/5$ for air. The force dF on the air plug is

$$dF = A\, dP = -\gamma Po\, A^2\, dx / V \tag{4}$$

so from dF=-k dx the spring constant k of the air in the volume V is

$$k = \gamma Po\, A^2 / V. \tag{5}$$

With the mass M given above, the resonant angular frequency ω of this mass-spring combination is given by

$$\omega^2 = \gamma \, Po \, A / (\rho \, V \, L). \tag{6}$$

Note that the squared resonant frequency depends on the A/L ratio of the port. A more complete analysis yields radiative end corrections to L: for a baffled end, we must add a length of 0.85 R, and for a free end, 0.61 R, where R is the tube radius [3].

When a port has a varying cross-sectional area, the analysis proceeds along different lines, since the air cannot be regarded as a simple cylindrical plug. We will work out the pressure change through the port by considering thin sections perpendicular to the port axis.

A symmetrical port with a gentle flare could be expressed using a number of different functions, but we will here use a hyperbolic cosine as a basis, so that the area of the port as a function of distance x along its axis is

$$A(x) = Ao \cosh(x / l), \tag{7}$$

where Ao is the area at the neck or throat, and l is the scale length of the flare. A real port might use this shape near the middle, but would smoothly "connect" it to the flat baffle of the speaker exterior. Nevertheless, acoustically the shape defined above is the relevant one, because the motion of the air becomes smaller and less important as the area increases. The varying area acts a a mechanical transformer to reduce the inertial effects of the air in the wider sections of the port. We can then downplay radiative end corrections, since the flared ends have little effect.

To calculate the resonance frequency of such a port with a closed volume V on one side, we can work out the pressure change along the axis through the port, assuming that a displacement Xo of the air occurs at the neck, at angular frequency ω. For the purpose of dealing with this lumped acoustic element, we can consider the air as incompressible. Thus the amplitude at position x is Xo Ao / A(x), and the acceleration will be $-\omega^2$ times this value. The pressure change dp to accelerate a thin disk of air of thickness dx will be

$$\begin{aligned} dp &= -\rho \, \omega^2 \, Xo \, dx \, Ao / A(x) \\ &= -\rho \, \omega^2 \, Xo \, dx / \cosh(x / l), \end{aligned} \tag{8}$$

and when integrated through the axis of the port from $-\infty$ to $+\infty$, the change in pressure p is

$$p = -\rho \, \omega^2 \, Xo \, \pi \, l. \tag{9}$$

The amount of air that flows through the port is Ao Xo, so the pressure change in the volume V is $-\gamma$ Po Ao Xo / V, where Po is atmospheric pressure. If we equate this pressure change to the value in the above equation, the resonance angular frequency ω becomes:

$$\omega^2 = \gamma \, Po \, Ao / (\rho \, \pi \, V \, l). \tag{10}$$

Except for the factor π, this is the same as the resonance frequency of a cylindrical port of area Ao and length l. Thus we can regard a port with shape given above as having an effective length π l. This assumes that the shape of the port conforms to cosh(x / l) sufficiently near the centre and that the ends do not significantly affect the result.

How large should Ao be for a port? The larger it is, the more the extraneous midrange sounds in the box (which might be produced by the distortion of the driver) will get out, and of course l needs to be adjusted with the dependences above to give the correct resonance frequency. If Ao is too small, the air velocity will be too high and causes turbulence, and the associated losses will increase. We normally want low losses so that the resonant enhancement of the port is limited mainly by the radiation load.

Pressure and Velocity Relationships

All the air that moves through a port must pass the throat, and for a compact source (size << wavelength) the retarded volume acceleration A(t) (m^3/sec^2) acts as the source of the external farfield pressure p at a distance r from the mouth, given for a baffled port by [4]

$$p = \rho\, A(t - r / c) / (2\, \pi\, r). \tag{11}$$

If Vo is the velocity amplitude in the throat of area Ao at angular frequency ω, then the amplitude of the volume acceleration is Ao ω Vo, leading the velocity by 90 degrees. Thus a measure of the sound pressure at a specific distance from the mouth allows us to obtain the throat velocity as

$$Vo = 2\, \pi\, r\, p / (\rho\, Ao\, \omega). \tag{12}$$

The pressure inside a loudspeaker box also bears a straightforward relationship to the velocity in the port and also the farfield pressure outside the box created by the port. Our basic premise is that the pressure outside the box is essentially negligible relative to the pressure in the box. We justify this later.

Fig. 1 shows a box with inside pressure P, a port of area Ao and length L with throat velocity v, and farfield pressure p at radius r. The acceleration a of the mass M = ρ Ao L of air in the port acted on by a force F = P Ao is

$$a = P\, Ao / (\rho\, Ao\, L) = P / (\rho\, L) \tag{13}$$

which does not depend on the throat area. Since the amplitudes of velocity and acceleration are related as a = ω v, where ω is the angular velocity, the velocity in the port is given by

$$v = P / (\omega\, \rho\, L). \tag{14}$$

The volume acceleration Ao a is the source for the farfield pressure as discussed earlier, and since the acceleration is directly proportional to the pressure P, we have for a baffled port opening

$$p = (Ao / L)\, P / (2 \pi r). \quad (15)$$

Aside from the distance factor, the Ao / L ratio of the port enters directly, and the outside pressure is (apart from retardation) exactly in phase with the box pressure.

It remains to justify that our earlier premise is reasonable. Naively we might think that a non-zero pressure just at the port mouth would discredit the theory above. If the length of the port is equal to the diameter (fairly short), and we set r about equal to R, the port radius, then substitution yields p ~ P / 4. But we have ignored the end corrections for the reactive radiation load on the two ends of the port, which take into account the pressure required to move the air at the ends. If we use the full effective length of the port, then the theory above works essentially with full box pressure at the port inner entrance and zero pressure at the equivalent port mouth, except for the very small resistive component of the radiation load, which really is negligible at bass frequencies with typical port diameters. Thus the theory presented above is indeed accurate if we include end corrections in the length L.

Other Shapes with Analytic Solutions

We can consider shapes other than cosh for the port cross-sectional area. Consider a hyperbolic shape in which the port radius R is given by

$$R^2 = Ro^2 + (\lambda x)^2 \quad (16)$$

which will give a cross-sectional area

$$A(x) = \pi (Ro^2 + (\lambda x)^2). \quad (17)$$

When we go through the same analysis as the cosh-shaped port, we find that the integral is tractable and the result for the effective length of the port is

$$L\_eff = pi\ Ro / \lambda. \quad (18)$$

We must interpret such formulae with care. Suppose we let λ go to infinity; then A(x) represents a hole of radius Ro in a wall, and the predicted L_eff is zero. However, the acoustic length will actually be finite due to reactive end effects which are not specifically included in the theory for L_eff, nor need they be, since the integral along the axis for the pressure drop for normal flares does not need an end correction.

Other shapes may give closed-form solutions as well, but there are some limits on the shape that become evident upon inspecting the integral to obtain the pressure across the port: the area A(x) must grow faster than x for large x, or else the integral diverges. What this means from a physical point of view is that for shapes whose area does not grow faster than x, the effective mass of the air in the port diverges. We would get a similar effect in a long pipe. The air could never diverge out into the open, and the pipe would display one-dimensional wave characteristics

in which the pressure would be in phase with the velocity and not the acceleration; it would not act as a lumped acoustic element. Short pipes do act as lumped elements; the phase difference between the ends is so small that we can consider the air as an incompressible plug.

Experimental Setup

The ports under test were mounted on a 25 l box which was driven by a large driver from the back, as shown in Fig. 2. One driver was an 18-inch high-compliance long-throw driver with a long voice coil in a relatively short magnetic gap, hence it is somewhat underdamped and of moderate efficiency. The other was a stiffer 12-inch long-throw unit with a large magnet structure, a long gap, and a short voice coil. This driver has heavy damping and is quite efficient, and it was used for most of the experiments to follow.

Some ports were flush-mounted on a large 4 x 4 feet baffle which was attached to the front of the box. In this way a close microphone (typically 10 cm away) can assess solely the output from the port, with no contamination from the rear-mounted driver. Other double-flanged and usually symmetric ports were bolted to the front of the box, and heavy cardboard baffling was affixed to the protruding port, again allowing an assessment of only the sound from the port. When the port outputs were blocked with rubber stoppers, the sound level at the microphone would fall by 30 dB, proving that the sound from the driver coming around the baffle was negligible. A test of a simple port at low levels confirmed that the acoustic signal from the port varied as 1/r, where r is the distance from the mouth. Typically, a distance of 10 cm was used. This was well within the critical distance for the room reverberation, so room modes play no part.

A low-distortion oscillator feeding a 150W/ch power amplifier was used to drive the system, and the current to the driver was monitored with a 0.1-ohm series resistor. Many experiments were carried out at 30 Hz, this being judged representative of actual use. Some of the smaller and longer ports were also tested at 15 Hz, this being done to allow higher air velocity with the 18-inch driver, which did not produce as high a box pressure. It is of course the box pressure that excites the port, and a 1/4-inch B&K type 4135 microphone was mounted in one side wall of the box to monitor this pressure. An available B&K type 4133 microphone was used to measure the output from the port. Although this is a free-field microphone, it has essentially a pressure response below 5 kHz.

A dual-channel data aquisition card with programmable anti-aliasing filters was used to capture two simultaneous channels of information. The sampling frequency was usually 5 kHz with the filters set just above 1 kHz, and records were 4096 samples long. Most of the interesting signals and noises from the ports were well below 1 kHz. Spectra of the time signals were derived by a 4096-point DFT with either a Hann window (for sharp peaks) or a 5-term flattop window (with very low scallop error for accurate peaks).

Pressure Bias

As the air speed through a port increases, the losses also increase, and there will be a proportionately higher oscillatory pressure drop across the port than at lower sound levels. If the

port is not symmetrical, then the losses will also not be symmetrical, and a static pressure difference can build up across the port. This does not of itself have a significant acoustic consequence, but it may cause the cone of the woofer to migrate away from its equilibrium position, and this may cause excess nonlinearity due to variations in Bl or suspension stiffness.

To test for such effects, an MKS Baratron differential pressure transducer was coupled to the inside of the box, referenced to atmospheric pressure outside the box. This transducer measures the deflection of a diaphragm capacitatively with a high-frequency balanced bridge, which is capable of responding to DC. Ports of various designs were tested at a variety of excitation levels.

Fig. 3 shows the box pressure versus speaker current for a port whose parameters are shown in the inset. The flare of the port exits to the outside, a very common design. We expected that the air would flow more easily from outside to the the inside of the port; the flare allowing the entering air to converge in gentle streamlines. For air flowing out of the box, the sharp inside edge would cause turbulence, while the flare does not seem able to spread out the streaming plume of air as it leaves. Thus we expected that the pressure in the box would rise. Surprisingly, although it does rise for high levels, at lower levels the pressure drop, though small, is actually reversed from our expectation.

When the port shown in Fig. 3 is slightly modified by a small step in the inner exit, as shown in dotted lines, the static pressure difference almost disappears. Thus it appears that port asymmetry is strongly influenced by small changes in the geometry of the air path.

A simple tube mounted flush with a box wall has only a slight asymmetry; the pressure in the box increases slightly with level. Such ports however tend to produce aerodynamic noise more easily than flared ports.

If sound levels are very high, then it is wise to symmetrize the port shape. Flares on both outer and inner ends assure this, and help to reduce port noise at intermediate levels. For large drivers, the suspension stiffness should not be too low, to prevent cone offsets.

Measurements of Air Flow

In order to study the airflow near a port, a hot-wire anemometer probe was constructed. A short length of #44 copper wire 8 mm long was soldered between the pointed ends of two copper rods 3 mm in diameter, and a current source of 1.0 A DC was applied by using a 10 VDC supply and a 10 ohm, 17 W resistor. The voltage across the probe was capacitor coupled to an amplifier and used as a signal somewhat proportional to air speed.

A plot of voltage versus current for the probe showed that the resistance at 1.0 A was 1.58 times that at room temperature. Since the resistance of a pure metal such as copper is closely proportional to the absolute temperature [273 + T(C)], the wire was about 200C at 1.0 A.

The wire loses heat mainly by convection, and moving air cools the wire, which changes the voltage across it. The probe is sensitive only to air speed, not direction, for motion perpendicular to the wire. The probe was not used for air motion along the wire, since the copper rods partially obstruct the air motion for this geometry, and air motion along the wire does not remove heat from the wire. Due to the small wire diameter, the probe is sensitive to quite high frequencies, probably well in excess of 1 kHz.

Corrections to the Simple Non-cylindrical Theory

The simple theory above for the cosh-shaped port ignores the curvature of the wavefront which must occur in the port. As the area increases, we have assumed that the relevant area is the section perpendicular to the axis, but in reality the acoustic signal must have a curvature, since the air at the edge must be moving along that edge, and not parallel to the central axis.

Fig. 4 shows that the effective area of the slice at distance x from the throat, which we model as A(x), must actually be somewhat less, since the curved fronts strike the port wall at a smaller radius than flat ones, even though they are curved. In the theory this manifests itself as an increase in the pressure across the port, since a reduced area means a larger acceleration, and hence more force. Meticulous measurements of a particular cosh-shaped port gave a throat radius of 1.86 cm and a scale length l = 3.50 cm. The associated box had a volume (with some corrections) of 5.36 litres. The predicted resonance frequency was 73.9 Hz, but measurement gave 69.7 Hz. This is a reasonable difference to ascribe to the curvature effect.

Results and Discussion

The port shapes studied included a long cosh-type, a short double flare, single flare, simple cylinder, complex moulded shapes from commercial speakers, and a cylinder with flared ends. There were several hundred data files, and in this paper we will discuss only selected topics which bear on the most interesting and salient points. The study is not complete, but the results do illuminate important factors.

Each of the graphs of microphone voltage shown in the figures can be converted to SPL. The pressures inside the box were monitored by a B&K type 4135 1/4 inch microphone with a preamp gain of 10 dB. To obtain box SPL in dB the reader can estimate the rms dBV from the graphs and add 133 dB. The external microphone was a B&K type 4133 1/2 inch, also with a preamp of 10 dB gain. This microphone was always mounted 10 cm from the mouth of the baffled port, and so its output would be 20 dB down a metre away. To obtain the SPL from the port at one metre, for 2π loading, add 101 dB to the rms dBV estimated from the graphs.

Fig. 5 shows the external microphone signal from a double-flared short port (denoted "scosh" for short-cosh) at 10 cm from the port mouth. The upper curve is on axis, and shows the chaotic fluctuations induced by the pulsating air stream from the port. Microphone orientation has a significant effect, and this measurement is clearly unacceptable. The middle curve shows the signal when a B&K windscreen is placed on the microphone. This is better, but some vestiges of blowing remain, and the amplitude is slightly reduced. The lower curve is the signal when the

microphone with no windscreen is 45 degrees off axis at the same distance from the port. The highly directed air stream has little deleterious effect now, and this measurement and the one taken along the baffle at the same distance are essentially the same. In the sequel we always use this latter position in order to measure the port output.

In the upper curve the microphone output is only corrupted during that phase of the oscillation when the air is streaming out of the port in a narrow plume. This has been checked by noting that this period coincides with positive box pressure. We interpret this to mean that the true acoustic output from a port is basically omnidirectional, so that it should not matter at what angle it is measured. But the excess kinetic energy in the airstream plays havoc with microphone diaphragms, so we must prevent such streaming motion from affecting the measurement. Note that the output from the two lower curves is about 0.25 Vrms, or -12 dBV. Thus the SPL at 1 metre from the mouth will be about -12 + 101 = 89 dB.

Fig. 6 shows the box and output pressure from a long, tapered cosh-shaped port ("lcosh") at moderately low levels. The upper curve of box pressure is almost perfectly in phase with the port output of the lower curve, as predicted by theory earlier. The volume acceleration is thus in phase with the box pressure, and the throat velocity would be lagging these two by 90 degrees. This port has a low loss at this level. As the loss goes up, the output pressure shows distortion and also starts to lead the box pressure, as shown in Fig. 7 for a short cylindrical port ("tube6"). The distortion waveform is reminiscent of slewing distortion. This example has almost the same output SPL as Fig. 6, but the sharp port edges cause turbulence and associated flow losses.

Fig. 8 shows microphone and probe signal voltages for the symmetrical flared short port (scosh). The upper curve is the pressure inside the box for a frequency of 30 Hz, and the middle curve shows the simultaneous anemometer output (increased air speed is up) for a position 10 cm from the port on its axis. Well outside the port, for positive box pressure a stream of air issues from the port in a narrow column, and cools the wire, while for negative box pressures the air outside comes in radially with much less velocity, and the wire rapidly heats up. The lower curve demonstrates the chaotic nature of the air flow; which can be felt by holding the hand in front of an overdriven port.

Fig. 9 shows data for the same port, driven a bit more gently. The upper curve is box pressure while the lower curve represents the air velocity with the anemometer probe placed precisely centrally in the throat. The hot wire is cooled every half cycle, so the signal is frequency doubled. When the probe is moved past the throat, the process inside the box is reversed in phase, and the stream of air occurs for a negative box pressure. We expect such a flow pattern for any port at high levels. When one places the hand near a port at high levels, it feels like a pump which is ejecting air. This is due to the narrow air stream, often only 10 degrees wide or less. The air must return through the port as well, of course, but it does so by converging towards the port in a much more orderly way, drawing air radially from a 2π solid angle. Of course during this period the stream is inside the box, and often affects the microphone which is monitoring box pressure; the fluctuations show up spectrally as a background on the otherwise relatively distortion-free oscillation from the cone.

Fig 10 shows how a short symmetrical port (scosh) behaves at 30 Hz as the drive level is increased. The current to the driver was 0.5, 1, 2, 3, and 4 amperes in the 5 steps shown from top to bottom. On the left is the port output pressure along the baffle at 10 cm, with scales +/- 2 V. On the right are the respective spectra, with the vertical axis spanning 120 dB. These levels have been chosen to display behaviour that is essentially linear at the top, progressing through to very high distortion at the bottom. As the level increases, third-order distortion rises sharply, and second-order distortion also rises markedly. If the port were truly symmetrical, one might not expect second-order to occur. But we are measuring on the outside of the box, so perhaps the flow, being asymmetric, is a cause, since the "half-wave-rectified" stream of air probably has some small effect on the acoustic pressure.

Curves for the highest excitation level are shown in Fig. 11. The upper curve is the box pressure, somewhat distorted, and the middle curve is an enlarged version of the output pressure. The sharp negative pressure spike in this signal occurs just after the peak of the box pressure waveform. The lower curve shows an overlay of the spectra at the extremes of Fig. 10. At the lowest level, the fundamental at 30 Hz is some 40 dB above the background. At the highest level, a factor of 8 in current, or 18 dB higher, the third harmonic is only 6 dB down, and the second about 15 dB down. Note especially that the spectrum background has risen by about 35 dB, and it has changed shape somewhat. This represents the fluctuations and aerodynamic noise from the port.

Results for a commercial moulded port with a gentle 90 degree bend are shown in Fig. 12. The upper curve is the box pressure (here about 150 dB SPL!), the middle curve is the port output, and its spectrum at the bottom. There are significant port losses, and the small oscillations, visible as a peak at about 700 Hz, probably represent resonances in the moulding that are being excited like a whistle. Were it not for the periodic reversal, a steady air flow of the same magnitude might cause real oscillation.

To indicate how a flared and an unflared port differ, the same sequences as in Fig. 10 are shown for two otherwise similar ports. Fig. 13 is for a short cylindrical port with sharp edges (tube6), and Fig. 14 is for a cylindrical port with flared ends of radius 1.8 cm ("sch"). The two ports have almost the same area and effective length. The flared port ironically tends to produce a sharper output pressure waveform, similar to the flared short port of Fig. 10. Perhaps there are less losses at edges, resulting in higher velocities. The turbulence of the sharp-edged port creates more loss, and this causes more compression in its behaviour at the highest levels. It also has more second-harmonic distortion, and this may be partly understood by the asymmetry of this port: its outside is on a flat baffle, but it protrudes unflanged into the box. The pressure bias of the port is not high, however, and this is also some measure of even-order distortion.

Lastly, Fig. 15 shows the compression characteristics of the three ports of Figs. 10 (scosh), Fig. 13 (tube6), Fig. 14 (sch), and the fourth long cosh-shaped port (lcosh), for a wider range of levels than shown in the figures. The data is generated by taking only the fundamental amplitude of both the box pressure and the output pressure. Interestingly, the long tapered port (lcosh) has a lower A/L ratio than the two cylindrical ports (tube6 & sch), but at high levels its output exceeds all the other ports, including the short flared port (scosh) which has the largest A/L ratio. The flared

cylindrical port (sch) actually shows increased output for intermediate levels, whereas its A/L companion the cylindrical port (tube6) displays a simple compression. It is possible that at even higher levels, the long tapered port will also turn over and exhibit an intermediate region of higher output before compression.

Some of the shapes in Fig. 15 may result from taking only the fundamental of the waveforms. The distortion in these waveforms is severe, yet the conclusions may not be altered even if other measures of performance are used.

Conclusion

It may have appeared from the earlier output waveforms that tapered or gently-flared ports are only slightly better than simple cut off pipes, but that would be too simplistic a view. We have not fully assessed ports with such gentle shapes, but perhaps the long tapered-port data shows that such ports hold out real promise. In addition, we have not really measured the loss in the ports under study except indirectly through the output curves, but these losses very much affect the net result when the ports are used as resonant bass enhancement components. The study should continue.

Acknowledgements

This project was first considered when the author spent four months at Bang and Olufsen in Denmark. Poul Praestgaard of B&O supplied some interesting ports to start this work. The author wishes to thank Cambridge speakers and TGI North America for supplying drivers to excite the test box. Doug Coote, an undergraduate project student, helped to fabricate some of the ports, set up the system, and run some early experiments. The author is grateful for research support from the Natural Sciences and Engineering Research Council of Canada.

References

1. N.Thiele and R.H.Small, *Vented-Box Loudspeaker Systems*, J. Audio Eng. Soc., Vol.21, 1973. Parts I-IV, June, July/Aug,Sept,Oct 1973.

2. Juha Backman, *The Nonlinear Behaviour of Reflex Ports*, presented at 98th AES Convention, Paris 1995 February 25-28, preprint # 3999.

3. L.L.Beranek, *Acoustics,* published by American Institute of Physics, 1986.

4. P.M.Morse, and K.U.Ingard, *Theoretical Acoustics*, Princeton Univ. Press, 1986, reprinted from McGraw Hill 1968 edition.

Figure Captions

1. Diagram to illustrate port parameters.

2. Test setup.

3. Pressure bias caused by an asymmetrical port, measured by a sensitive differential pressure gauge which responds to DC.

4. Diagram illustrating the curved acoustic wavefronts which reduce the effective cross-sectional area of a slice of the port.

5. Microphone signal from a short, cosh-shaped port. The upper trace is the output on axis 10 cm from the port mouth, and shows the effects of the streaming air. The middle trace is the same location with a windscreen fitted to the microphone. The lower trace is the output at 45 degrees from the axis at the same distance, and it is essentially the same as the result along the baffle.

6. Microphone signals from inside and outside the test box. The upper trace trace is inside, the lower outside, showing the inphase character of these signals when a port has a gentle taper with a low loss.

7. The same as Fig.6, but for a short cylindrical port with some loss, at about the same acoustic output. The output pressure now leads in phase, as would be expected if the losses tend to make the port velocity in phase with the box pressure.

8. Microphone and anemometer probe signals from a short, flared port. The upper trace is box pressure, the middle is air velocity on axis 10 cm from the mouth, while the lower trace shows the same signal over a longer time span, indicating the chaotic nature of the air flow.

9. Microphone and probe signals from the same port as Fig.8. The upper is box pressure, and the lower is the probe output when it is placed precisely in the throat centre of the port. The airflow is now symmetrical, resulting in a frequency doubling of the probe output.

10. A sequence of microphone port output signals and their spectra for a short flared port for increasing drive levels. The output shows both second- and third-harmonic distortion, and output compression at the higher levels.

11. Microphone signals and spectra for the same port as in Fig.10. The upper trace is box pressure, and the middle trace is output, at the highest level of Fig.10. The lower traces are spectral overlays.of the highest and lowest levels of Fig.10.

12. Signals from a commercial moulded port. The upper trace is box pressure and the middle is output, with the spectrum in the bottom trace. This port shows small oscillations which show up as a peak in the spectrum at about 700 Hz. The port is highly overdriven.

13. A sequence of output signals and spectra similar to Fig.10, but for a short, cylindrical port with sharp edges. The second-harmonic distortion at the highest level rivals the also-high third-harmonic distortion.

14. A sequence again similar to Fig.10, but for a short cylindrical port with both ends flared to a radius of 1.8 cm. The output actually shows sharper features, but the compression is less.

15. Showing the output fundamental pressure versus box fundamental pressure for the three ports of Figs. 10, 13 and 14, and a fourth long tapered port. The highest compression is shown by the port with the sharp edges, while the long tapered port actually performs best at high levels. It is not clear by what mechanism some ports actually have enhanced output at intermediate levels.

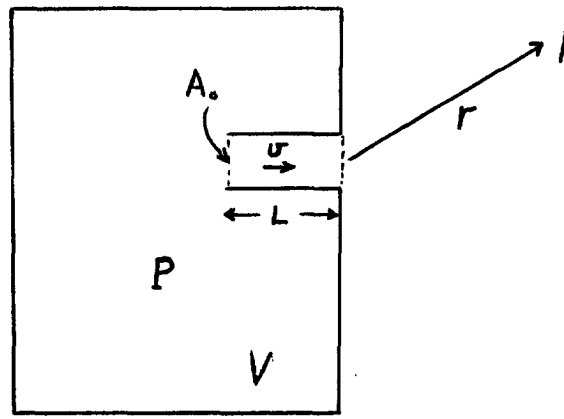

Figure 1

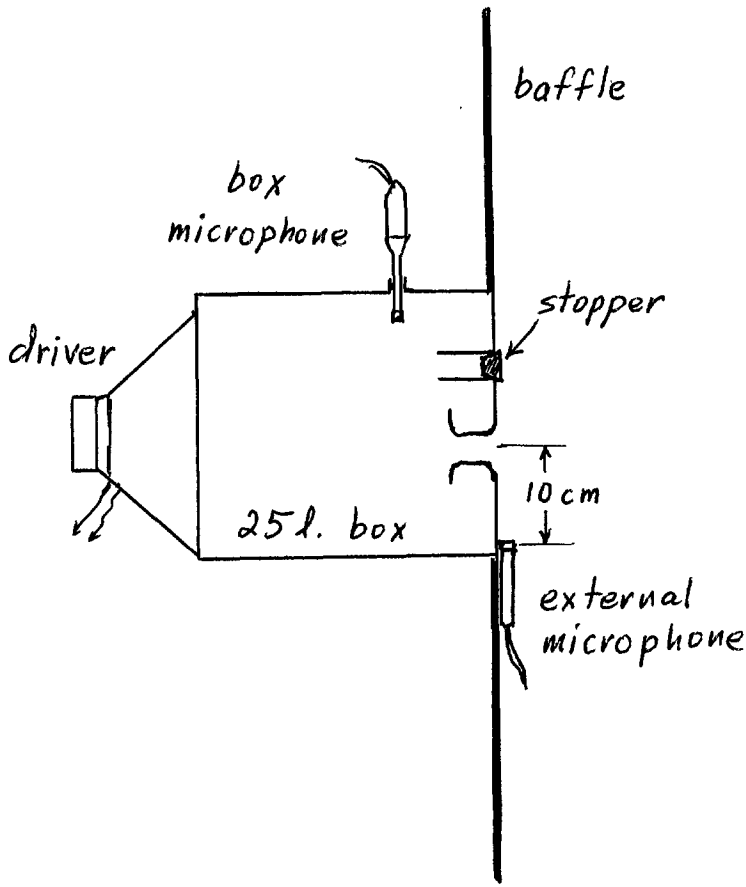
baffle
box
microphone
stopper
driver
10 cm
25 l. box
external
microphone

Figure 2

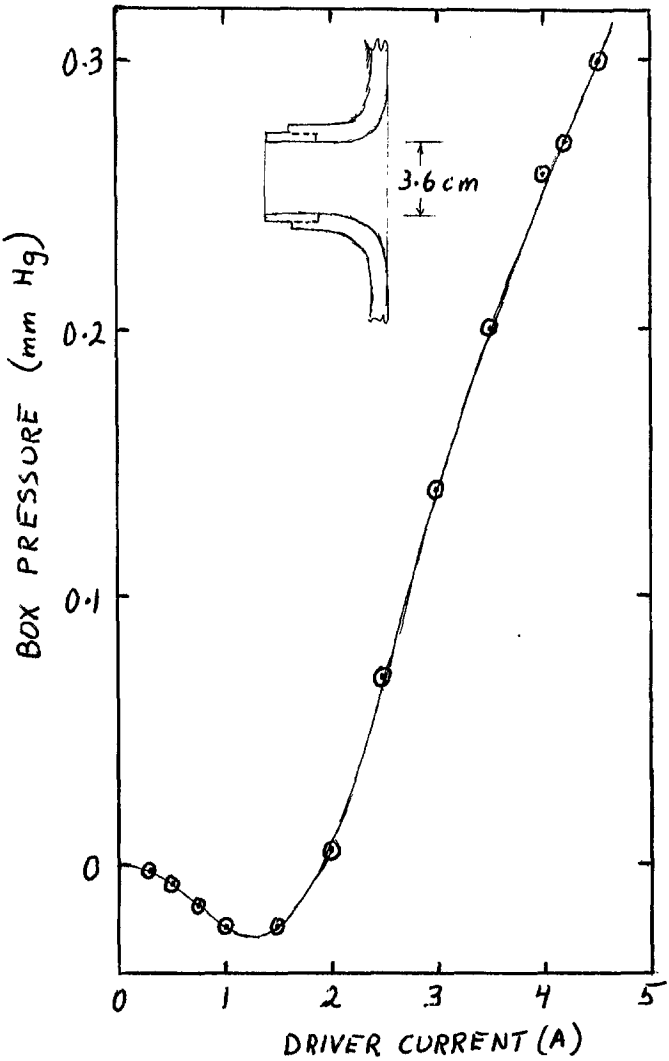

Figure 3

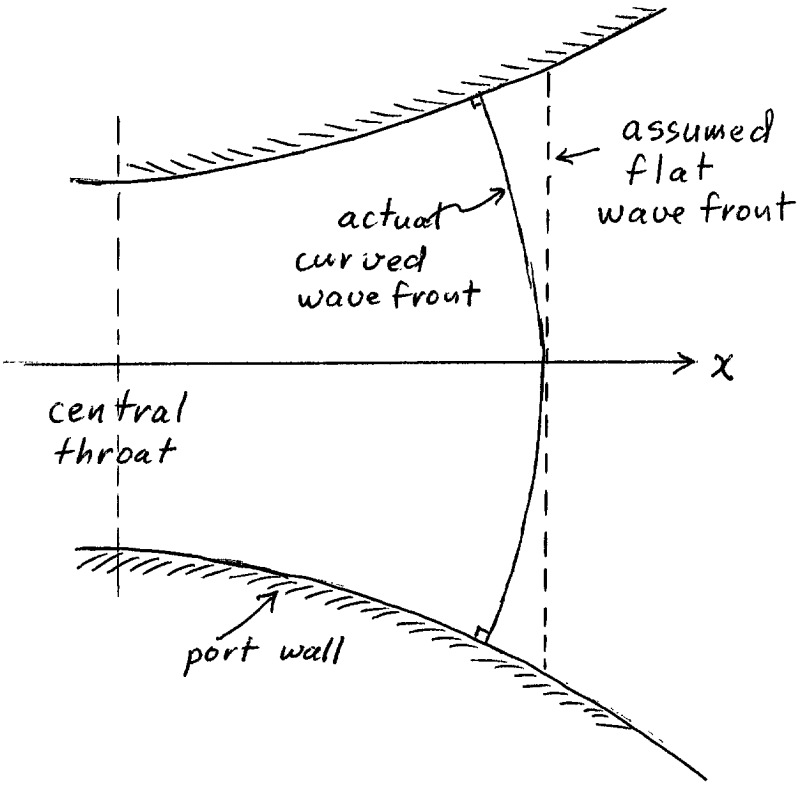
assumed
flat
wave front
actual
curved
wave front
x
central
throat
port wall

Figure 4

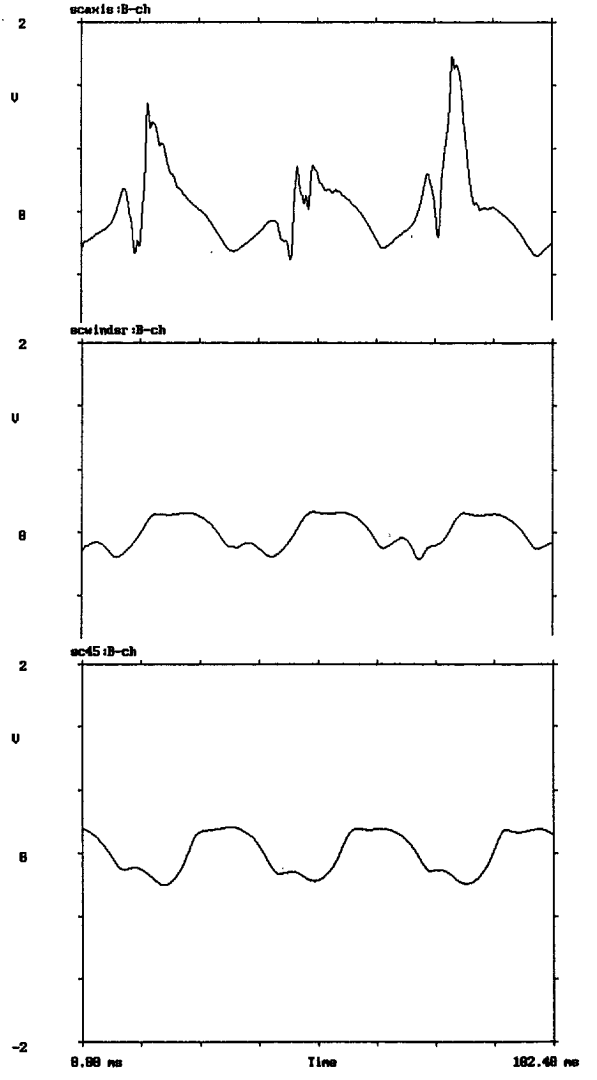
scaxis:B-ch
2
V
0
scwindsr:B-ch
2
V
0
sc45:B-ch
2
V
0
-2
0.00 ms
Time
102.40 ms

Figure 5

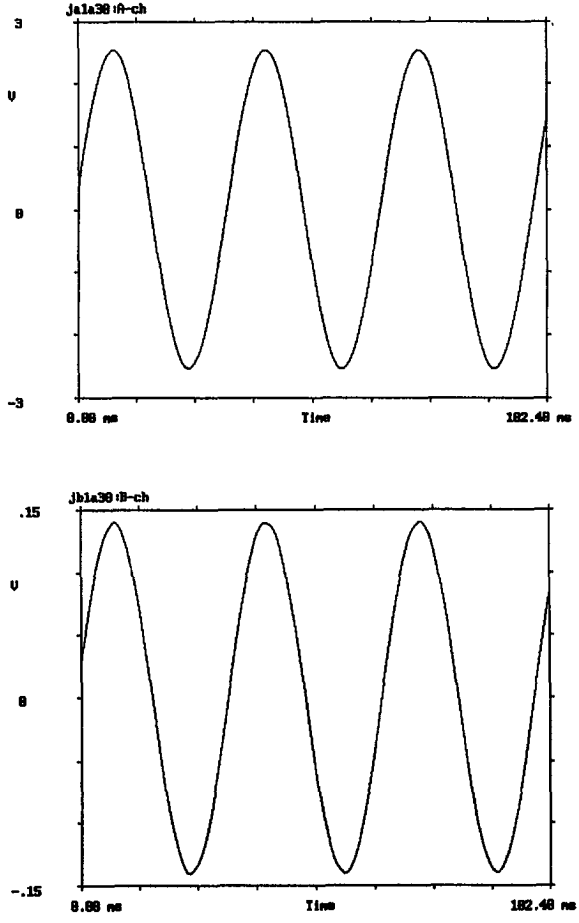
ja1a30:A-ch
3
V
0
-3
0.00 ms
Time
182.48 ms
jb1a30:B-ch
.15
V
0
-.15
0.00 ms
Time
182.48 ms

Figure 6

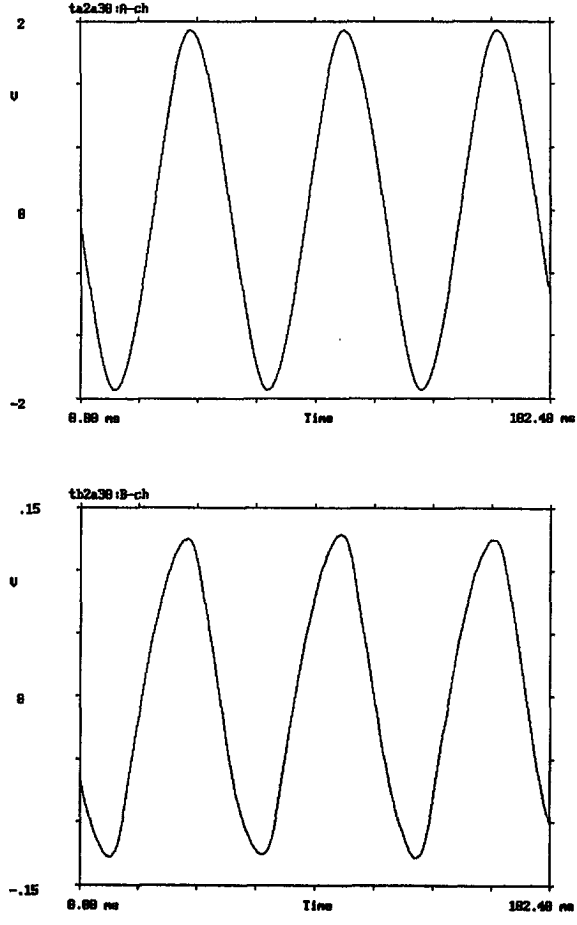
ta2a38:A-ch
2
V
0
-2
0.00 ms
Time
182.48 ms
tb2a38:B-ch
.15
V
0
-.15
0.00 ms
Time
182.48 ms

Figure 7

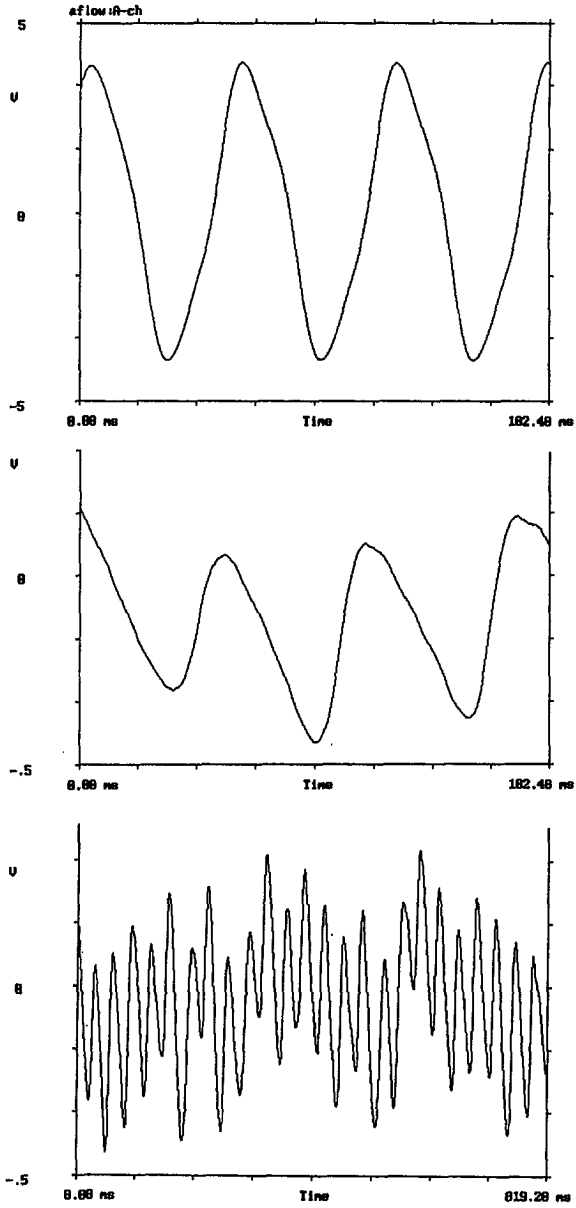
aflow:A-ch
5
V
0
-5
0.00 ms
Time
182.40 ms
V
0
-.5
0.00 ms
Time
182.40 ms
V
0
-.5
0.00 ms
Time
819.20 ms

Figure 8

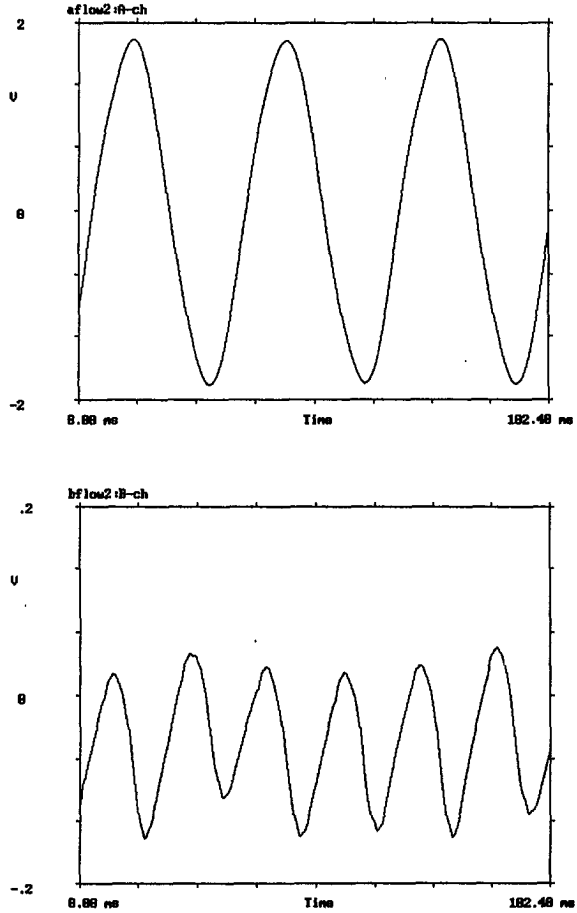
aflow2:A-ch
2
V
0
-2
8.00 ms
Time
182.40 ms
bflow2:B-ch
.2
V
0
-.2
8.00 ms
Time
182.40 ms

Figure 9

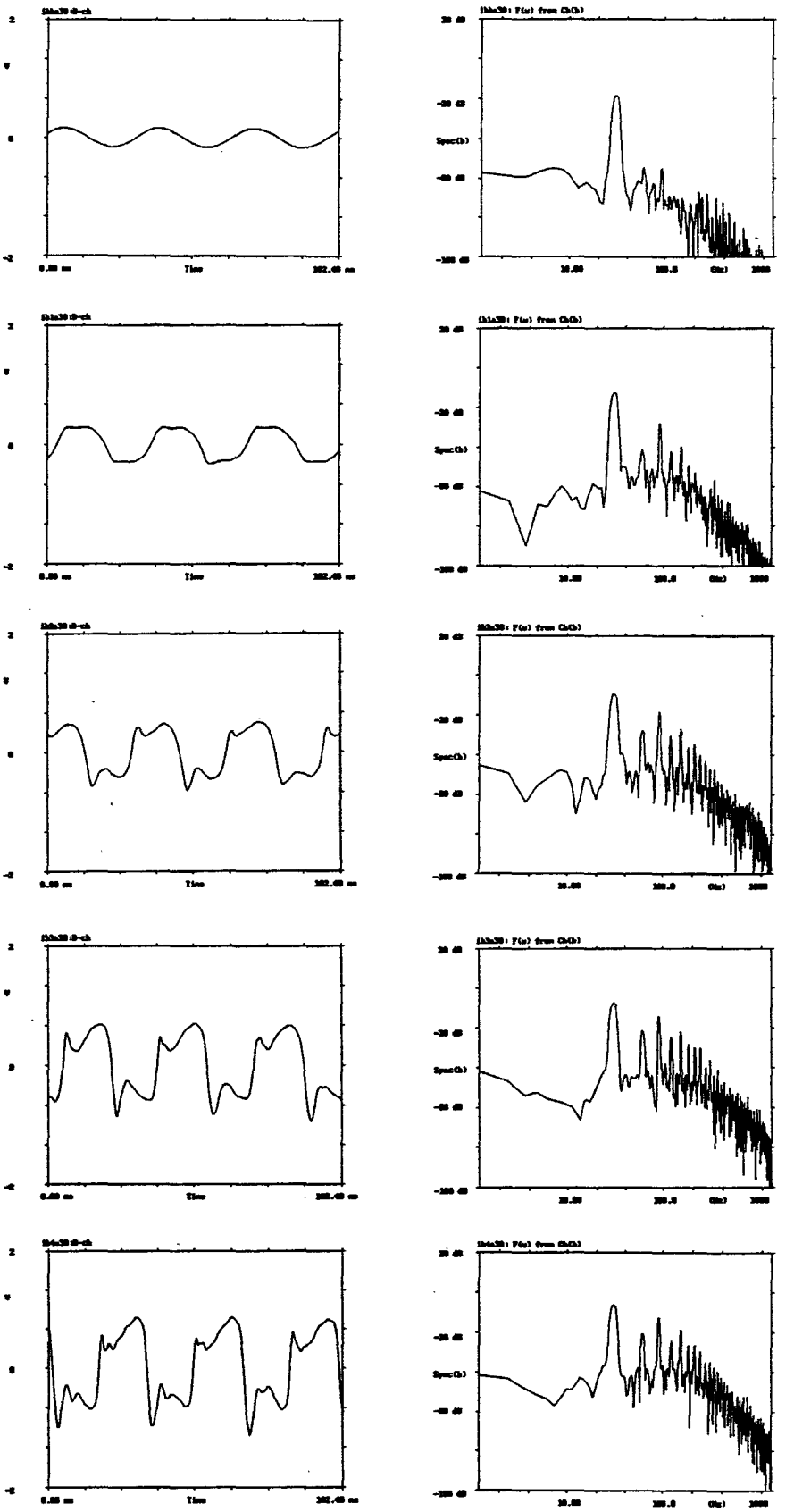

Figure 10

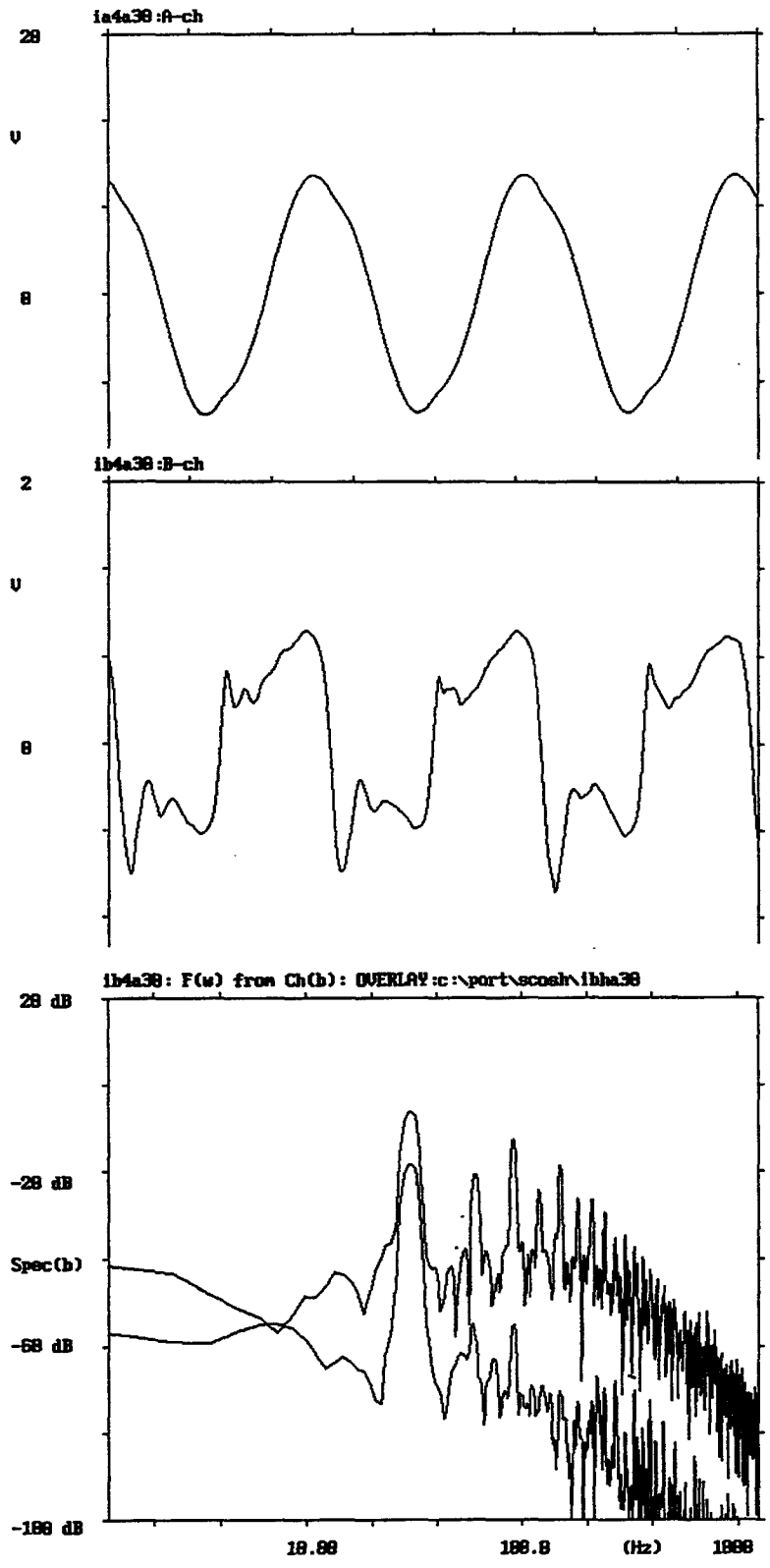
ia4a30:A-ch
20
V
0
ib4a30:B-ch
2
V
0
ib4a30: F(w) from Ch(b): OVERLAY:c:\port\scosh\ibha30
20 dB
-20 dB
Spec(b)
-60 dB
-100 dB
10.00
100.0
(Hz)
1000

Figure 11

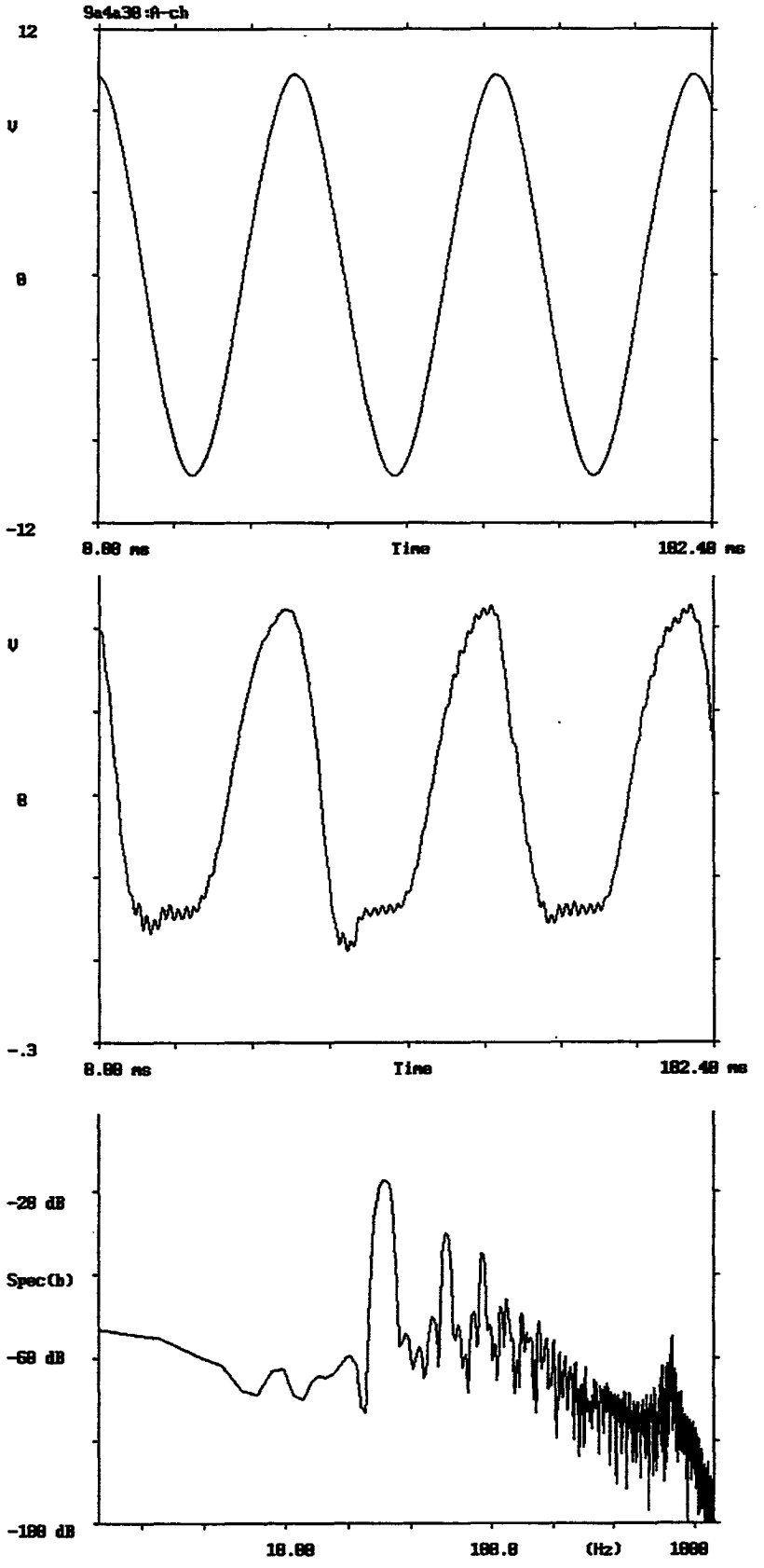
9a4a38:A-ch
12
V
0
-12
0.00 ms
Time
182.48 ms
V
0
-.3
0.00 ms
Time
182.48 ms
-20 dB
Spec(b)
-60 dB
-100 dB
10.00
100.0
(Hz)
1000

Figure 12

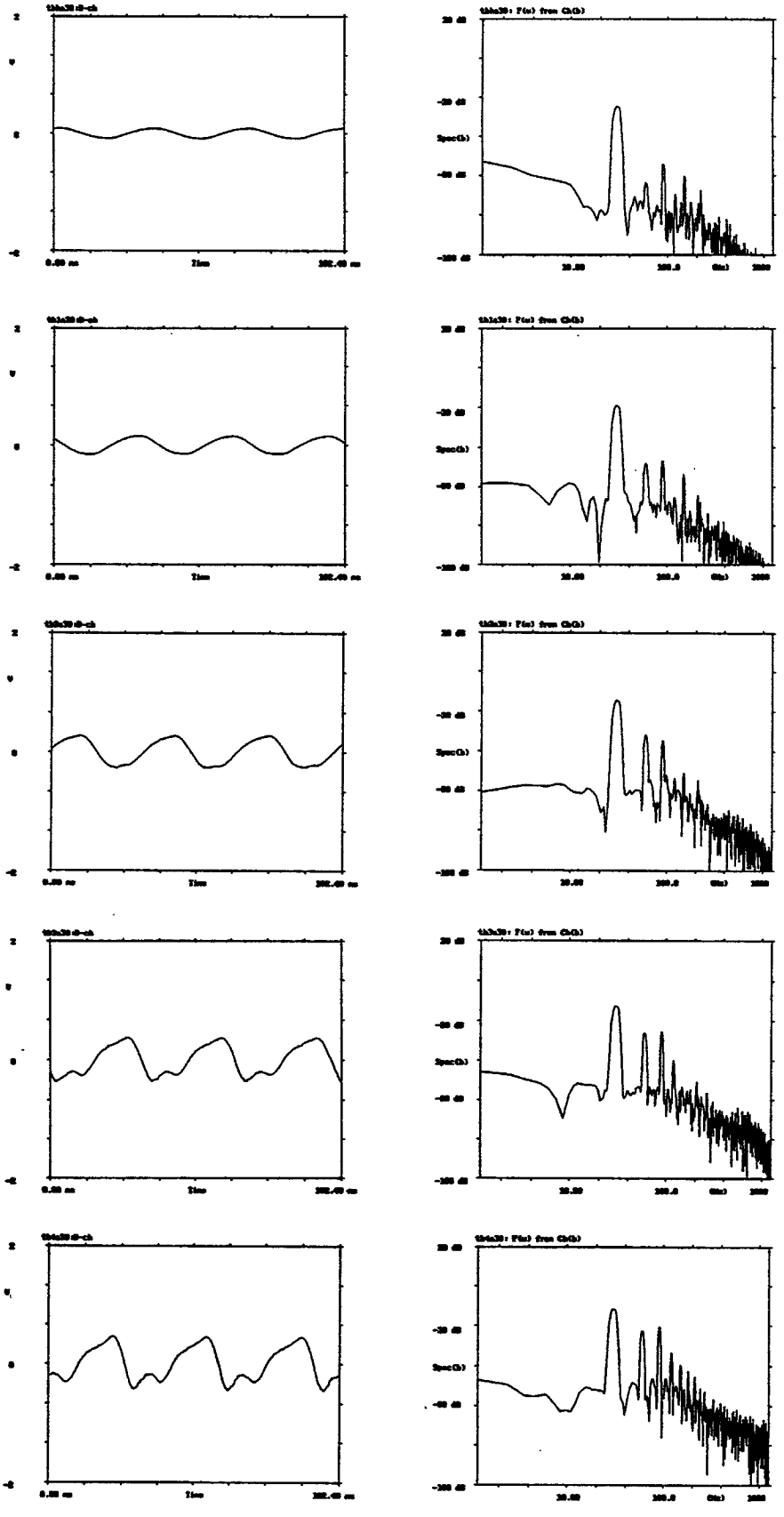

Figure 13

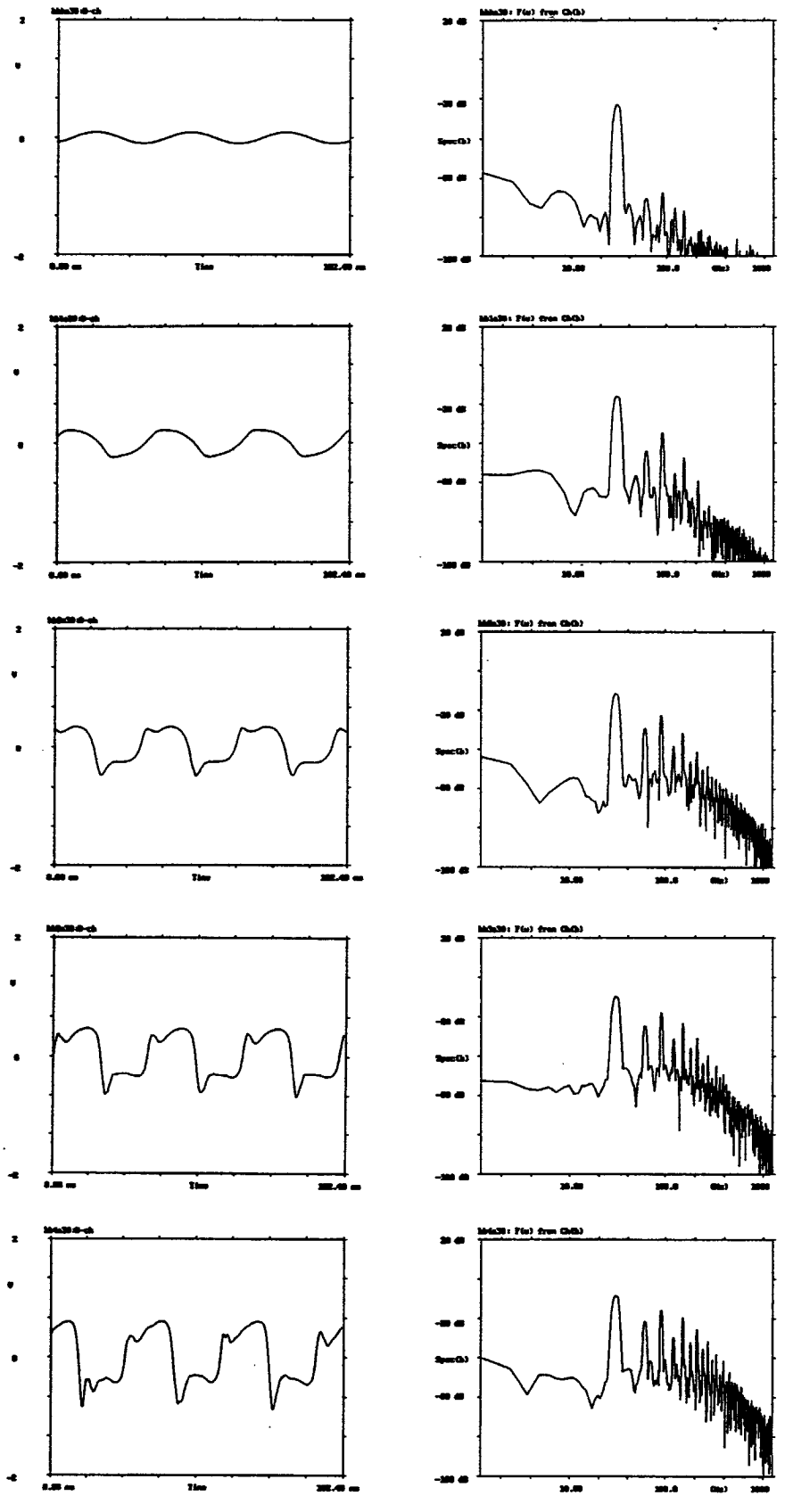

Figure 14

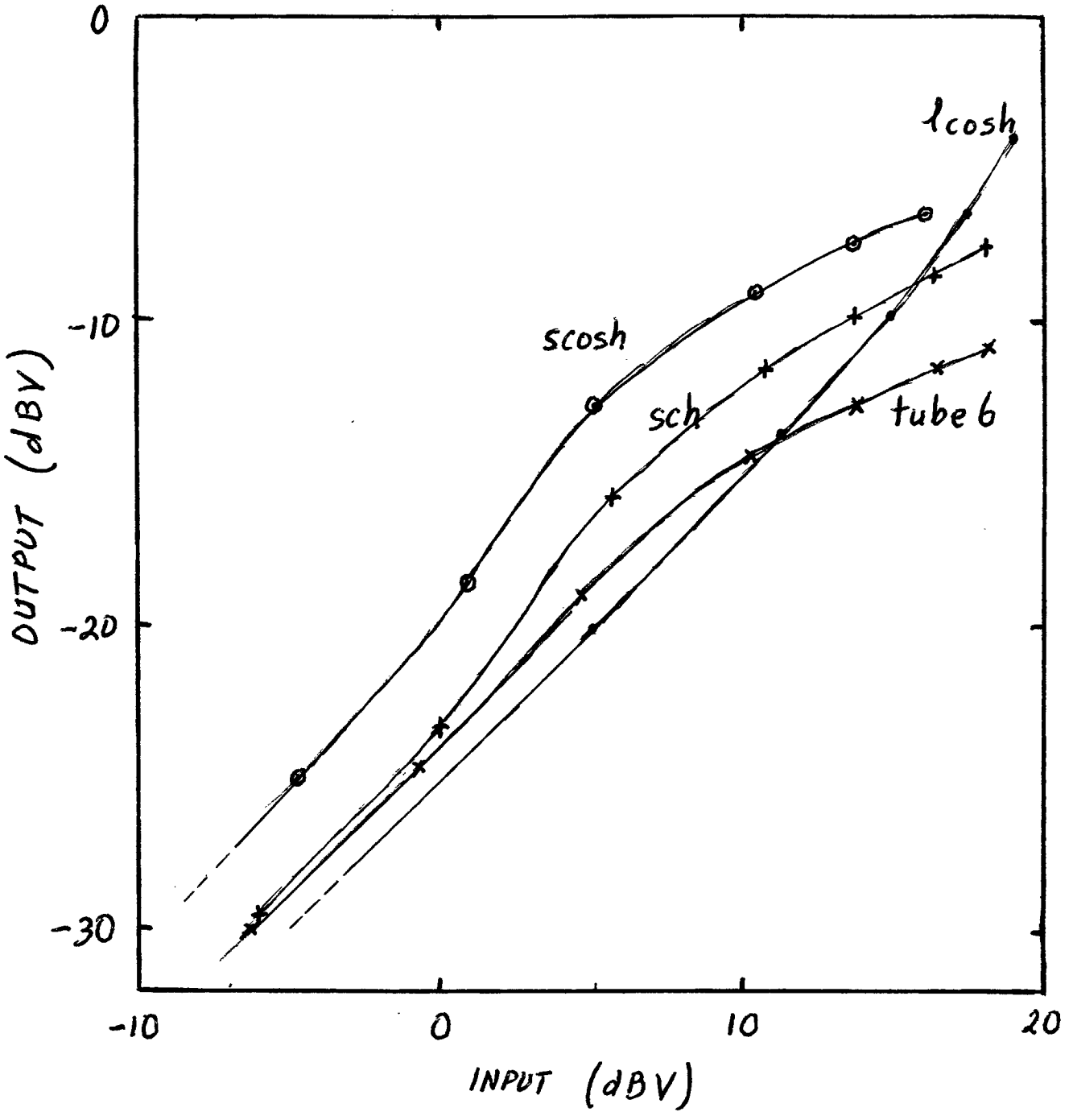

Figure 15